https://doi.org/10.5194/egusphere-2024-3594
Preprint. Discussion started: 22 November 2024

Double dating in the Middle Pleistocene: assessing the consistency and performance of the carbonate U–Th and U–Pb dating methods

Timothy J. Pollard[1], Jon D. Woodhead[1], Russell N. Drysdale[1], R. Lawrence Edwards[2], Xianglei Li[3], Ashlea N. Wainwright[1], Mathieu Pythoud[2], Hai Cheng[4,5], John C. Hellstrom[1], Ilaria Isola[6], Eleonora Regattieri[7], Giovanni Zanchetta[8], and Dylan S. Parmenter[2]

[1]School of Geography, Earth and Atmospheric Sciences, University of Melbourne, Parkville, Victoria, Australia
[2]Department of Earth and Environmental Sciences, University of Minnesota, Minneapolis, MN, USA
[3]Institute of Vertebrate Paleontology and Paleoanthropology, Chinese Academy of Science, Beijing, China
[4]Institute of Global Environmental Change, Xi'an Jiaotong University, Xi'an, Shaanxi, China
[5]State Key Laboratory of Loess and Quaternary Geology, Institute of Earth Environment, Chinese Academy of Sciences, Xi'an, Shaanxi, China
[6]Istituto di Geoscienze e Georisorse, IGG-CNR, Pisa, Italy
[7]Istituto Nazionale di Geofisica e Vulcanologia INGV, Pisa, Italy
[8]Department of Earth Sciences, University of Pisa, Pisa, Italy

Correspondence: Timothy J. Pollard (timothy.pollard@student.unimelb.edu.au)

Abstract.

The U–Th and U–Pb dating methods are widely used for radiometric dating of Pleistocene carbonates, such as speleothems and corals. The U–Th dating method has been incrementally refined over recent decades, largely through advances in mass spectrometry, and is now capable of providing accurate and precise ages for carbonates as old as 640 ka in ideal circumstances. Likewise, the U–Pb method, which was previously used exclusively for dating pre-Quaternary materials, has been adapted in recent times for dating carbonates as young as a few hundred ka. As a result, there is now considerable overlap in the applicable range of these two dating methods but, as yet, little data available regarding their consistency or relative performance when dating samples within this age range. In this study we undertake a systematic comparison of the U–Th and U–Pb dating methods focusing on a large part of their potential overlapping age range (∼430–630 ka). We achieve this by 'double dating' speleothems (secondary cave mineral deposits) from Corchia Cave, central Italy, that are well-suited to both methods and adopt state-of-the-art isotope dilution MC-ICP-MS analytical protocols. This includes a U–Th measurement protocol that collects the low abundance $^{234}U^{+}$ and $^{230}Th^{+}$ ion beams in a Faraday cup fitted with a 10^{13} Ω resistor, a protocol that is not only ideally suited to dating samples within this age range, but also permits measurement of $^{238}U/^{235}U$ ratios at a level of accuracy and precision appropriate for assessing natural $^{238}U/^{235}U$ variability.

The results of this comparison demonstrate excellent agreement between the U–Th and U–Pb dating methods and show that both methods are capable of producing accurate and precise ages over this interval. We find that U–Pb age uncertainties are

https://doi.org/10.5194/egusphere-2024-3594
Preprint. Discussion started: 22 November 2024

generally less predictable than U–Th age uncertainties, but on average do not increase significantly over the age interval considered, whereas U–Th age uncertainties tend to increase in a more predictable (approximately exponential) manner. Furthermore, U–Pb age uncertainties are highly dependent on the availability of sub-samples with a substantial spread in Pb/U ratios and/or highly 'radiogenic' (i.e. very low inherited-Pb) material. We also find that average U–Pb isochron age precision surpasses that of U–Th age determinations at ca. 520 ka, although the exact age overlap point is expected to vary significantly across different sample types and study sites. Overall, these findings support the prospect of obtaining accurate and internally consistent U-series based chronologies spanning the Middle Pleistocene and beyond, and suggest that for some carbonate samples the U–Pb chronometer may provide superior age precision to the U–Th chronometer prior to the latter reaching its upper age limit.

1 Introduction

Geochronologists have access to a wide range of radiometric dating tools for tracking Earth and planetary processes. The utility of each is constrained predominantly by the material under study and its elemental composition, in particular the proportion of parent and daughter nuclides present and their half-lives, which, together, define a useful range of application. Deciding which chronometer to use in a particular situation is usually relatively straightforward, for example, in dating organic samples of ∼55 ka or less, radiocarbon dating is the clear method of choice (e.g. Hajdas et al., 2021). In some cases, however, two or more chronometers may be applicable to a given situation and, here, determining the optimal dating approach requires careful consideration, especially if both methods are close to the limits of their applicable range. This is the case for the carbonate U–Th and U–Pb chronometers, which exhibit potential overlap throughout a substantial part of the Middle Pleistocene (ca. 400–650 ka).

The U–Th and U–Pb dating methods are widely employed for radiometric dating of Pleistocene carbonates and provide some of the most accurate and precise ages over this interval. For example, the application of U–Th dating to carbonates, such as speleothems (secondary cave mineral deposits) and corals, has led to fundamental advances in our understanding of Quaternary palaeoclimate (e.g. Edwards et al., 2003; Fairchild and Baker, 2012). It has provided some of the most accurate and precise constraints on the timing of major climate events throughout the last ∼640 ka, including, for example, glacial terminations (Cheng et al., 2016) and millennial-scale climate perturbations associated with Dansgaard-Oeschger events (Corrick et al., 2020). The U–Th chronometer is by far the most widely applied carbonate dating method and has been used to successfully date samples ranging in age from several years (e.g. Shen et al., 2012) back to ∼640 ka (Cheng et al., 2016), at which point the chronometer loses its age resolving power as ^{230}Th approaches secular equilibrium with its parent isotope ^{238}U.

More recently, the long-established U–Pb geochronometer has been adapted for dating Quaternary carbonates and offers a valuable means of extending speleothem and coral chronologies beyond the ∼650-ka limit imposed by the U–Th technique (Richards et al., 1998; Woodhead et al., 2006; Denniston et al., 2008; Klaus et al., 2017). U–Pb geochronology is based on in-growth of the radiogenic isotopes ^{206}Pb and ^{207}Pb from their respective radioactive 'parents' ^{238}U and ^{235}U, via a series of shorter-lived intermediate 'daughter' isotopes. The U–Pb chronometer is currently less widely applied to carbonates than the

https://doi.org/10.5194/egusphere-2024-3594
Preprint. Discussion started: 22 November 2024

U–Th chronometer, but is of similar utility, having, for example, provided radiometric age constraints on the timing of Early Pleistocene glacial terminations (Bajo et al., 2020), the age of key hominin fossils (Walker et al., 2006; Pickering et al., 2011), and chronologies for sub-arctic permafrost thawing over the past ∼1.5 Ma (Vaks et al., 2020). Although the U–Pb method is nominally better suited to dating older materials where sufficient time has passed for relatively large amounts of radiogenic Pb to accumulate, it is also well suited to dating Middle Pleistocene materials, which typically have [^{234}U/^{238}U] values (where square brackets denote an activity ratio) that are analytically resolvable from radioactive equilibrium, thus facilitating a precise disequilibrium correction (Woodhead et al., 2006). In ideal circumstances the carbonate U–Pb geochronometer can also provide precise ages for materials as young as ∼200 ka (Cliff et al., 2010).

Traditionally, the U–Th chronometer has been the method of choice for dating carbonates throughout the entirety of its applicable age range. However, for some samples, it is conceivable that the U–Pb method may perform equally well, or even better, as the U–Th chronometer approaches its upper age limit. Therefore, when dating carbonate samples in the age range of ca. 400–650 ka, choosing an optimal dating approach requires some consideration. In practical terms, the U–Th method may be considered advantageous because it usually involves the analysis of single samples extracted from discrete positions within a given speleothem or coral sample and is thus less labour intensive on a per-age basis. The U–Pb method, on the other hand, typically involves isochron dating approaches whereby multiple sub-samples from within an individual growth domain are analysed to compute a single age. Although isochron approaches are more labour intensive, they also provide a first-order check on the assumption of closed-system behaviour and more accurately account for any initial (non-radiogenic) quantity of the daughter isotopes. Additional considerations in applying the U–Pb chronometer to Pleistocene samples include its reliance on assumptions regarding the initial state of the intermediate daughter products ^{231}Pa and ^{226}Ra and closed-system behaviour with respect to intermediate products beyond ^{230}Th in the ^{238}U decay series, such as ^{222}Rn (Richards et al., 1998).

In terms of age precision, the relative merits of each chronometer are not yet well characterised for samples approaching the limits of their applicable age ranges (i.e. upper limit with respect to U–Th, and lower limit with respect to U–Pb). It may be expected that, for 'well-behaved' samples, the precision of the U–Pb chronometer would surpass that of U–Th somewhere prior to the latter reaching its nominal upper age limit. The exact point at which this occurs is difficult to establish *a priori*, however, because the precision of U–Pb isochron ages is not a simple function of the analytical precision on individual isotope ratio measurements (e.g Woodhead et al., 2012; Engel and Pickering, 2022). Direct comparison of samples dated using both methods thus provides an appropriate means of characterising their relative performance in terms of age precision, and of assessing their consistency.

Previous studies have compared carbonate samples dated by both the U–Th and U–Pb chronometers, although these have tended to include a relatively small number of samples spanning a limited age range. For example, Richards et al. (1998) and Pickering et al. (2010) both 'double dated' young speleothem samples (<260 ka) using the U–Th and U–Pb methods and found good general agreement between the two. However, in both of these studies a lack of precision on one or both of the dating methods precluded a more definitive finding. Cliff et al. (2010) undertook a more detailed comparison, obtaining multiple U–

https://doi.org/10.5194/egusphere-2024-3594
Preprint. Discussion started: 22 November 2024

Th and U–Pb ages for a flowstone that grew between approximately 350–265 ka, and found good agreement for the youngest growth segment, although age agreement for the middle and older growth segments was more equivocal. While this study was more comprehensive than previous comparisons, it also had some limitations. For example, only one full isochron age was included in the age comparison and there was some uncertainty in co-registering the U–Th and U–Pb ages to a common depth scale, which precluded a more statistically rigorous comparison.

In this study we present a comparison of U–Th and U–Pb chronometers focussing on the older part of their overlapping age range (ca. 430–630 ka), where routine application of the U–Pb chronometer is a more realistic prospect. We achieve this by 'double dating' carbonate speleothem samples using both methods and assess consistency between the two chronometers and their relative merits in terms of age precision and other practical considerations. In contrast to previous comparisons, we compute full U–Pb Tera-Wasserburg (Tera and Wasserburg, 1972) isochron ages for all samples and adopt a state-of-the-art MC-ICP-MS based analytical protocols. This includes an all-Faraday-cup U–Th measurement protocol that employs a ^{233}U-^{236}U double spike for mass bias correction (e.g. Andersen et al., 2004; Potter et al., 2005; Cheng et al., 2013), and collects the low abundance ^{234}U and ^{230}Th isotopes in a Faraday cup fitted with a 10^{13} Ω resistor, which offers superior signal-to-noise ratios relative to more conventional 10^{11} Ω resistors (Pythoud, 2022). Use of this analytical protocol allows age consistency to be assessed more rigorously than in previous studies and facilitates an assessment of age precision using the most appropriate U–Th measurement protocol currently available for samples of this age.

2 Study site and samples

The speleothem samples analysed in this study were collected from Corchia Cave, located in the Alpi Apuane massif of Central Italy (43°59'N, 10°13'E). This cave system, which is developed in Mesozoic marbles, dolomitic marbles and dolomites, is one of the longest (∼60 km) and deepest (∼1250 m) in Europe and has been the subject of extensive past cave exploration (Piccini et al., 2008) and scientific study (e.g. Drysdale et al., 2004; Zanchetta et al., 2007; Bajo et al., 2017; Drysdale et al., 2019; Isola et al., 2019). The cave site receives the majority of its high annual precipitation (∼2500 mm yr-1) from eastward moving air masses originating over the North Atlantic Ocean, resulting in a coupling between large-scale surface ocean conditions in the North Atlantic and geochemical signals preserved in speleothems at the site (e.g. Drysdale et al., 2020). Owing largely to this linkage, Corchia Cave has yielded an abundance of palaeoclimate data of regional and global significance, including precise constraints on the timing of glacial terminations (Drysdale et al., 2009; Bajo et al., 2020) and interglacial climate variability (Regattieri et al., 2014; Tzedakis et al., 2018).

Palaeoclimate reconstruction studies undertaken at Corchia Cave have largely focussed on stalagmites collected from the large and well-decorated Galleria delle Stalattiti. This chamber sits approximately 400 m vertically below the surface, at an elevation of 835 m above sea level, and about 800 m from the nearest natural cave opening (Piccini et al., 2008). The microclimate of Galleria delle Stalattiti is relatively stable, typical of deep-cave environments, with a humidity consistently above 98% and an average present-day temperature of 7.9 °C (Drysdale et al., 2019). Stalagmites from this chamber are typically well

https://doi.org/10.5194/egusphere-2024-3594
Preprint. Discussion started: 22 November 2024

suited to U-series geochronology with consistently high U content (typically 3–20 ppm) and very low detrital Th, as well as relatively low inherited Pb (Bajo et al., 2012). Furthermore, most stalagmites are composed of clean (i.e. free of visible detritus) compact columnar calcite, which is typically associated with the preservation of primary geochemical signals and closed-system behaviour with respect to U-series nuclides (e.g. Fairchild et al., 2006; Scholz et al., 2014). These characteristics make stalagmites from the Galleria delle Stalattiti very well-suited to U-series geochronology, and when combined with the site's suitability for palaeoclimate reconstruction, have led to a large number of U–Th and U–Pb determinations being undertaken on materials from the site. These data suggests that initial [$^{234}U/^{238}U$] values of speleothems from this cave chamber are always less than 1 and have undergone a long-term evolution over the past several hundred kyr towards more ^{234}U-depleted values (Woodhead et al., 2006), with values as low as ∼0.65 obtained for Late Holocene materials (Zanchetta et al., 2007).

This study focusses on three stalagmites (sample IDs: CCB, CC2/CC15, and CC17-1) that were found broken near their original in situ position during field campaigns between 2001 and 2017. These stalagmites are large, with lengths of 67–130 cm, and average diameters ranging from approximately 9–22 cm. Following collection, the stalagmites were halved along their vertical growth axes and polished to aid in identifying visible growth laminations. In section, the stalagmites are white to grey in colour and predominately composed of compact translucent-to-opaque primary calcite. Exceptions are the very top of CCB, which contains some slightly porous calcite as the diameter tapers toward the tip, and the middle of CC17-1, which contains some localised, slightly porous sections associated with sharp changes in growth axis direction. These features are atypical of Galleria delle Stalattiti speleothems and were avoided during sampling.

3 Analytical methods

3.1 Sampling

Samples for both U–Th and U–Pb dating were extracted using a dental drill, targeting clean and compact calcite by carefully tracing along visible growth contours approximately 5 mm apart at the central axis but tapering along the flanks. Several solid sub-samples of ∼4 mm (width) × ∼4 mm (length) × ∼3 mm (depth), or 20–120 mg, were then extracted from each growth domain. For each sampling position, one sub-sample taken from the centre of the isochron was used for U–Th analysis and the remaining 5–10 sub-samples were used for U–Pb analysis. The only exception to this is sample CC17-1-3, where the U–Th sample was taken from a growth layer marginally below that of the corresponding U–Pb samples, however, this sampling offset was negligible relative to the age of these growth layers.

3.2 U–Th geochronology

U–Th dating was performed using a modified version of the all-Faraday-cup mass spectrometry protocol of Cheng et al. (2013), but with the $^{234}U^{+}$ and $^{230}Th^{+}$ ion beams collected in a Faraday cup fitted with a 10^{13} Ω resistor (Pythoud, 2022). Chemistry procedures were similar to those described in Edwards et al. (1987). Briefly, solid samples of 20–110 mg (equivalent to ∼500 ng U) were dissolved in ∼1% HNO_3 before addition of a mixed ^{233}U- ^{236}U-^{229}Th tracer calibrated against IRMM-074/10

https://doi.org/10.5194/egusphere-2024-3594
Preprint. Discussion started: 22 November 2024

(Cheng et al., 2013). Approximately six drops of concentrated $HClO_4$ were added to each sample beaker before being capped and refluxed on a hotplate for several hours to ensure complete sample-spike equilibration. Following complete dry down, separation and purification of U and Th proceeded in two stages. Firstly, U and Th were separated from the matrix using Fe co-precipitation in 2 N HCl by drop-wise addition of NH_4OH followed by centrifuging. Secondly, U and Th were separated and further purified via elution chromatography using BioRad AG1-X8 anion exchange resin, with the Th fraction collected in 6 N HCl and the U fraction collected in ultra-pure H_2O. The Th fraction was then passed through a second identical column to ensure complete separation from U. Following this, the purified U and Th sample fractions were dried down and sequentially treated with $HClO_4$ and HNO_3 to oxidise any remaining organics, before being taken up in 1% HNO_3 for analysis.

The U and Th isotope ratios were measured separately in static mode on a Thermo-Scientific Neptune Plus MC-ICP-MS (see The Supplement for details on the detector configuration). Samples were introduced into the mass spectrometer via a Cetac Aridus II desolvating-nebulising system fitted with a C50 PFA concentric nebuliser, using an uptake rate of 30–50 μL min-1. Zeros were measured for 13 minutes for both U and Th immediately prior to sample introduction. U measurements were then made over 5–10 minutes with a $^{234}U^{+}$ signal size between 8–18 mV. Th measurements immediately followed U for each sample and were made over 1–5 minutes with a $^{230}Th^{+}$ signal size between 8–20 mV.

For Faraday cups fitted with 10^{10} Ω and 10^{11} Ω resistors, amplifier gain calibration was performed via the mass spectrometer software using a standard current at the start of each run. However, the low dynamic range of the 10^{13} Ω resistor precluded use of this approach for the cup fitted with this resistor. Therefore, amplifier gain on this detector was characterised by periodic (∼fortnightly) measurement of Nd standard SRM 3135a following Pythoud (2022). Tailing of the $^{238}U^{+}$ and $^{235}U^{+}$ ion beams were characterised by analysis of un-spiked CRM-112A prior to each run, with the background measured at masses 233, 233.5, 234.5, 236 and 237 amu on the axial SEM with the Retarding Potential Quadrupole (RPQ) off. A logarithmic regression fit through these data was then used to estimate tailing onto the mass 233–236 cups as a function of the signal intensity at mass 237 (Pythoud, 2022). For each U fraction, tailing was corrected by measuring the background at mass 237 on the axial SEM during sample analysis and applying the predicted $M_{\mathrm{tail}}/237$ ratios (where M refers to masses 233–236). Tailing of the $^{232}Th^{+}$ beam onto the mass 230 cup was negligible given the very high $^{230}Th/^{232}Th$ ratios of the samples analysed in this study and was not corrected for.

Data reduction was performed using an offline spreadsheet that implements a tau correction following Pythoud (2022) to account for the slow response time of 10^{13} Ω resistors, before applying the ^{238}U tail correction as described above, and mass bias correction based on the exponential law (Russell et al., 1978) using the $^{233}U/^{236}U$ ratio measured for each sample. The mass bias factor calculated for the U fraction was subsequently used to correct the Th fraction run immediately after, based on the assumption of near-equivalent mass bias behaviour between U and Th isotopes (Potter et al., 2005; Cheng et al., 2013). This is justified by the consistent mass bias behaviour observed on this instrument, especially over multiple successive analyses (Pythoud, 2022). Finally, corrected U ratios were normalised to CRM-112A, which was periodically analysed throughout each run. U–Th ages and uncertainties (Table 1) were then computed using a Python script that calculates age uncertainties via

https://doi.org/10.5194/egusphere-2024-3594
Preprint. Discussion started: 22 November 2024

Table 1. U–Th dating results.

Sample ID	U (ppm)	$\delta^{234}U^{1}$ (‰)	$[^{230}Th/^{238}U]$	$[^{230}Th/^{232}Th]$	Age (ka)^{2}	Age 95% CI (ka)^{3}	$\delta^{234}U_{initial}$ (‰)
CCB-B-1	18.05	−85.94±0.32	0.86499±0.00034	1.30× 10^{6}	433.3±4.4	(429.0, 437.8)	−291.9±4.5
CCB-C-3	8.10	−84.01±0.28	0.86925±0.00037	1.96× 10^{5}	447.8±4.9	(442.9, 452.7)	−297.3±4.8
CCB-C-1	7.23	−80.93±0.29	0.87390±0.00041	1.17× 10^{5}	452.1±5.4	(446.9, 457.7)	−289.9±5.1
CCB-C-20	11.36	−80.10±0.25	0.87532±0.00026	2.22× 10^{6}	455.0±4.2	(450.9, 459.4)	−289.3±4.2
CC17-1-1	5.11	−91.45±0.28	0.86025±0.00046	1.78× 10^{5}	459.4±6.5	(453.2, 466.2)	−334.4±6.8
CC17-1-35	3.51	−82.39±0.29	0.87545±0.00027	7.73× 10^{4}	495.0±7.3	(488.0, 502.4)	−333.0±7.8
CCB-E-9	7.53	−66.94±0.22	0.89801±0.00019	3.19× 10^{5}	513.4±8.8	(507.9, 520.0)	−285.1±8.3
CCB-E-10	6.84	−63.60±0.26	0.90340±0.00022	9.56× 10^{5}	527.0±8.1	(519.3, 535.4)	−281.4±7.4
CCB-F-16	6.96	−61.39±0.27	0.90664±0.00030	4.00× 10^{5}	530.1±9.2	(521.4, 539.9)	−274.0±8.1
CCB-F-1	5.38	−60.26±0.31	0.90843±0.00039	5.67× 10^{5}	534.4±11.4	(523.8, 546.7)	−272.3±9.8
CC2-1	7.10	−62.32±0.18	0.90650±0.00026	2.04× 10^{6}	555.6±9.0	(547.0, 564.9)	−298.9±8.2
CCB-6-1	7.43	−50.75±0.37	0.92490±0.00026	1.01× 10^{6}	628.0±29.1	(603.3, 661.6)	−298.6±26.8
CC17-1-3	4.53	−57.57±0.35	0.91440±0.00033	2.97× 10^{5}	592.2±21.2	(573.4, 615.8)	−306.2±20.0
CC15-1	3.36	−48.70±0.34	0.92789±0.00037	7.14× 10^{5}	632.4±31.5	(606.0, 669.1)	−290.1±28.0

Uncertainties are given at the 2σ level unless otherwise specified. Decay constant values: $\lambda_{238} = 1.55125 \times 10^{-10}$ (Jaffey et al., 1971) and $\lambda_{234} = 2.82206 \times 10^{-6}$ (Cheng et al., 2013), and $\lambda_{230} = 9.1705 \times 10^{-6}$ (Cheng et al., 2013). [1] $\delta^{234}U = \left[^{234}U/^{238}U\right] - 1$. [2] Uncertainties calculated by first-order analytical error propagation (e.g. Ludwig and Titterington, 1994). [3] Calculated by Monte Carlo simulation.

both analytical (Ludwig and Titterington, 1994) and Monte Carlo approaches (e.g. Hellstrom, 1998; Ludwig, 2003) (see The Supplement for further details). For the purposes of comparison with the U–Pb ages, a correction for initial ^{230}Th was not applied to the U–Th ages, although given the very high ^{230}Th/^{232}Th ratios of these samples, such a correction would have a negligible effect on calculated ages and uncertainties.

3.3 U–Pb geochronology

Analytical methods for U–Pb geochronology built on those published previously (e.g. Woodhead et al., 2006, 2012; Sniderman et al., 2016) but using the streamlined chemistry procedure described in Engel et al. (2020). Solid calcite samples were repeatedly cleaned by brief (∼1 min) immersion in dilute (∼0.01 M) multiply-distilled HCl, followed by washing in ultrapure water, before drying in a HEPA-filtered laminar flow hood. The cleaned samples were then individually weighed into pre-cleaned Teflon beakers and treated with sufficient 6 N HCl to ensure complete dissolution. A mixed ^{233}U–^{205}Pb isotopic tracer, calibrated against EarthTime reference solutions (Condon et al., 2015), was then weighed into the vials and each one sealed and refluxed on the hotplate for several hours to ensure complete sample-spike equilibration. Samples were then dried down and U and Pb separated from the calcite matrix using the single-column mixed-resin ion-exchange technique described in Engel et al. (2020).

https://doi.org/10.5194/egusphere-2024-3594
Preprint. Discussion started: 22 November 2024

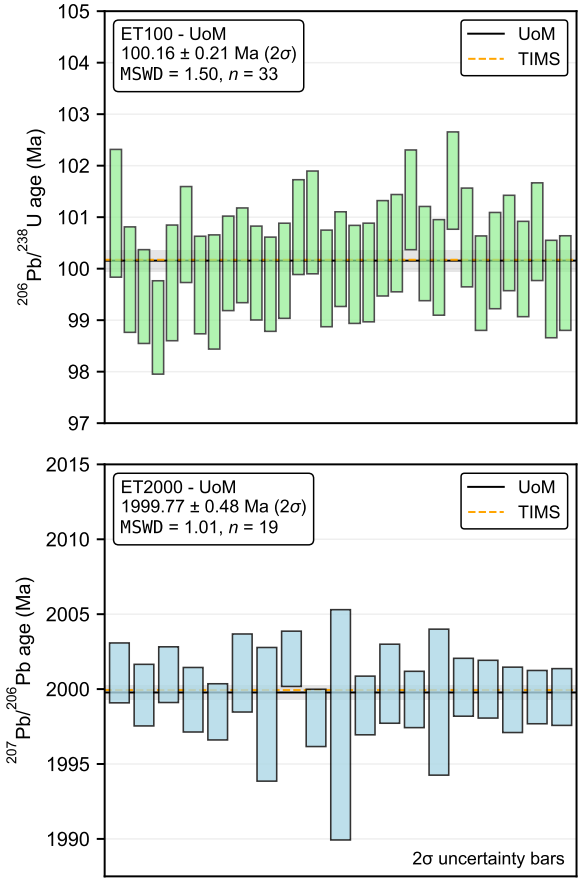

Figure 1. Radiogenic $^{206}Pb/^{238}U$ and $^{207}Pb/^{206}Pb$ age determinations for EarthTime (ET) 'synthetic zircon' standards analysed during the course of this study using a similar Pb load to the speleothem samples and identical column chemistry and mass spectrometry procedures. The weighted average age is plotted as the black line with grey shading indicating the 95% confidence interval. Also shown for comparison are the average inter-laboratory TIMS ages obtained by Schaltegger et al. (2021). $^{207}Pb/^{206}Pb$ ages were calculated with $^{238}U/^{235}U = 137.818$.

Isotope ratios were measured on a Nu Plasma MC–ICP-MS using a DSN-100 desolvation unit and MicroMist glass nebuliser, operating with an uptake rate of ~80 μL min-1. Instrumental mass bias effects were monitored and corrected using NIST SRM 981 reference material in the case of Pb, and the sample's internal $^{238}U/^{235}U$ ratio in the case of U.

U–Pb isochron regression lines were fitted using `DQPB` (Pollard et al., 2023), initially employing the `spine` robust isochron algorithm (Powell et al., 2020). This algorithm accounts for analytical uncertainties and can accommodate datasets with weighted residuals that depart from a strict Gaussian distribution, but converges to the classical least-squares solution of York et al. (2004) for 'well behaved' datasets. The spine-width, s, was used to assess suitability of this algorithm for each dataset in relation to the upper 95% confidence limit on s (here denoted s_{lim}) obtained by simulation of Gaussian distributed datasets (Powell et al.,

https://doi.org/10.5194/egusphere-2024-3594
Preprint. Discussion started: 22 November 2024

2020). In cases where s clearly exceeded this upper limit the Robust Model 2 (`RM2`) algorithm outlined in Pollard et al. (2023) was implemented instead. This regression algorithm ignores analytical uncertainties, deriving a robust dispersion scale from the data itself rather than assigned analytical uncertainties, and is thus generally better suited to data sets containing significant 'excess scatter' (i.e. scatter in excess of that attributable to assigned analytical uncertainties). However, for isochrons where s only marginally exceeded the upper 95% confidence limit, the `spine` algorithm was considered likely to provide a more accurate best-fit line than the `RM2` algorithm, although in this case the `spine` uncertainty calculations become potentially unreliable. Thus, where s exceeded s_{lim} by less than an arbitrary but reasonable value of 50% the `spine` regression line was retained, but uncertainties were expanded in an attempt to accommodate data scatter above what is reasonably accounted for by measurement uncertainties. This was achieved by multiplying the covariance matrix of the slope and y-intercept, $\mathbf{V}_\theta$, by $(s/s_{\mathrm{lim}})^2$. Implementing the `RM2` algorithm instead for these datasets does not significantly alter any of the conclusions of this study.

U–Pb ages were calculated as the intercept point between the regression line and disequilibrium concordia curve on a Tera-Wasserburg diagram (e.g. Wendt and Carl, 1985), incorporating the measured [^{234}U/^{238}U] value from the U–Th analysis into the iterative age-solving procedure, and assuming initial [^{230}Th/^{238}U], [^{231}Pa/^{235}U], [^{226}Ra/^{238}U] values equal to 0 (Fig. 2). Uncertainties were calculated using a Python script that implements the Monte Carlo simulation approach described in Pollard et al. (2023) with 10^6 iterations (see The Supplement for further details).

For the purpose of determining analytical accuracy, each U–Pb session included analysis of several 'synthetic zircon' standards: ET-100Ma, ET-500Ma, and ET-2Ga (Fig. 1). These materials, produced by the EarthTime initiative, have nominal U and Pb compositions approximating zircons with the ages of 100 Ma, 500 Ma, and 2 Ga, but without any matrix (Condon et al., 2008). While they were originally conceived for quality control during TIMS single zircon analysis, and are still routinely used for that purpose (e.g Zhong et al., 2017; Szymanowski and Schoene, 2020), they are also ideally suited to isotope dilution (ID) carbonate U–Pb studies since the quantities of U and Pb being analysed can be controlled to approximate unknowns and the highly radiogenic nature of the Pb involved serves to rapidly identify any anomalous analytical issues, such as unexpected high blanks. In our studies, we pass aliquots of these solutions (typically equating to ∼5 ng of radiogenic Pb) through the same column chemistry as our samples.

4 Results and discussion

4.1 Age consistency

We first assessed consistency between the two chronometers on a pairwise basis. To assess if the U–Th and U– Pb ages for each sample agreed within their analytical uncertainties, we performed a simple hypothesis test (a Z-test), which amounted to testing if differences between the ages were consistent with zero while accounting for analytical uncertainties (e.g Barlow, 1989). In most cases, analytical uncertainties could reasonably be assumed to conform to a Gaussian distribution for both the U–Th and

https://doi.org/10.5194/egusphere-2024-3594
Preprint. Discussion started: 22 November 2024

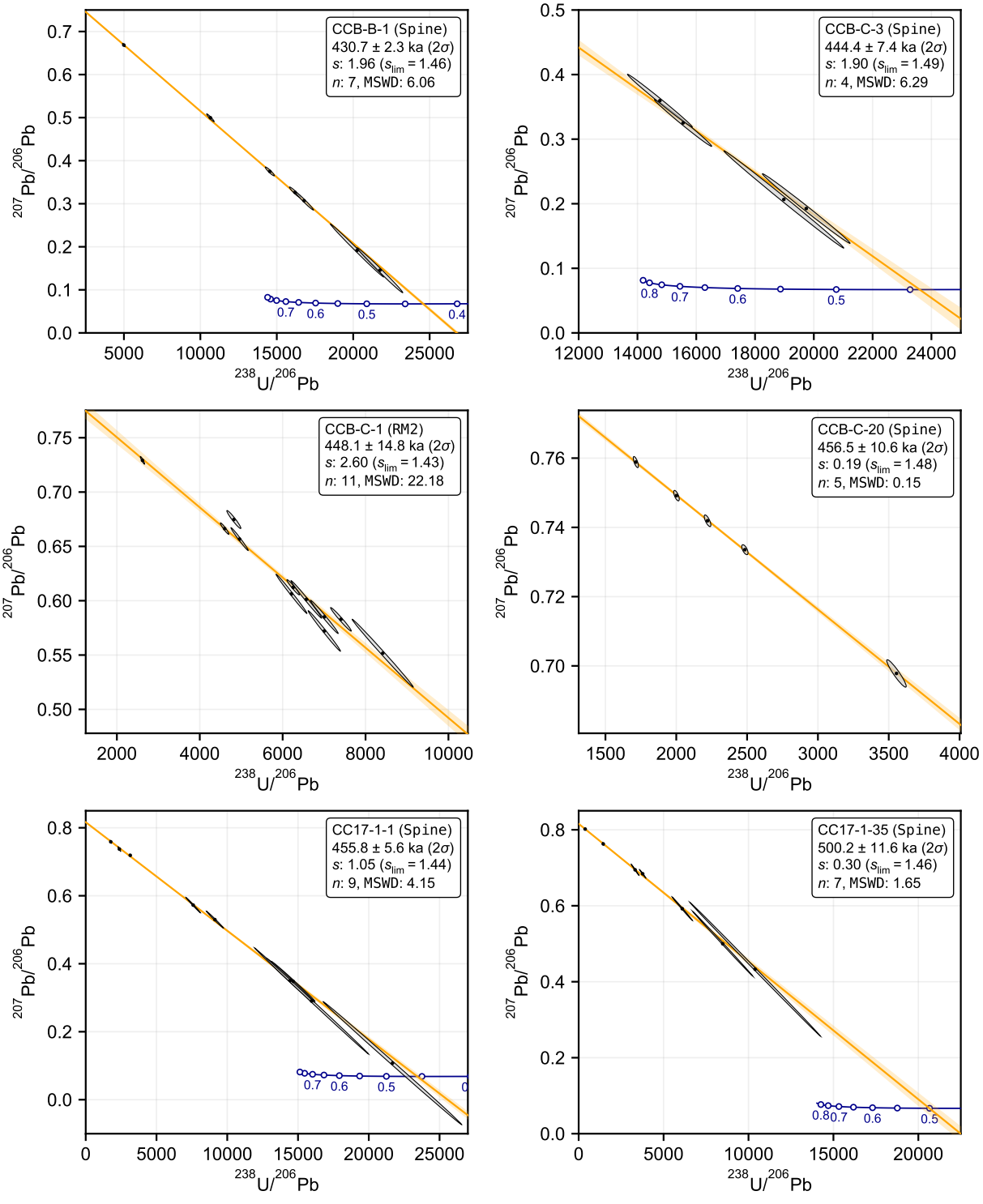

https://doi.org/10.5194/egusphere-2024-3594
Preprint. Discussion started: 22 November 2024

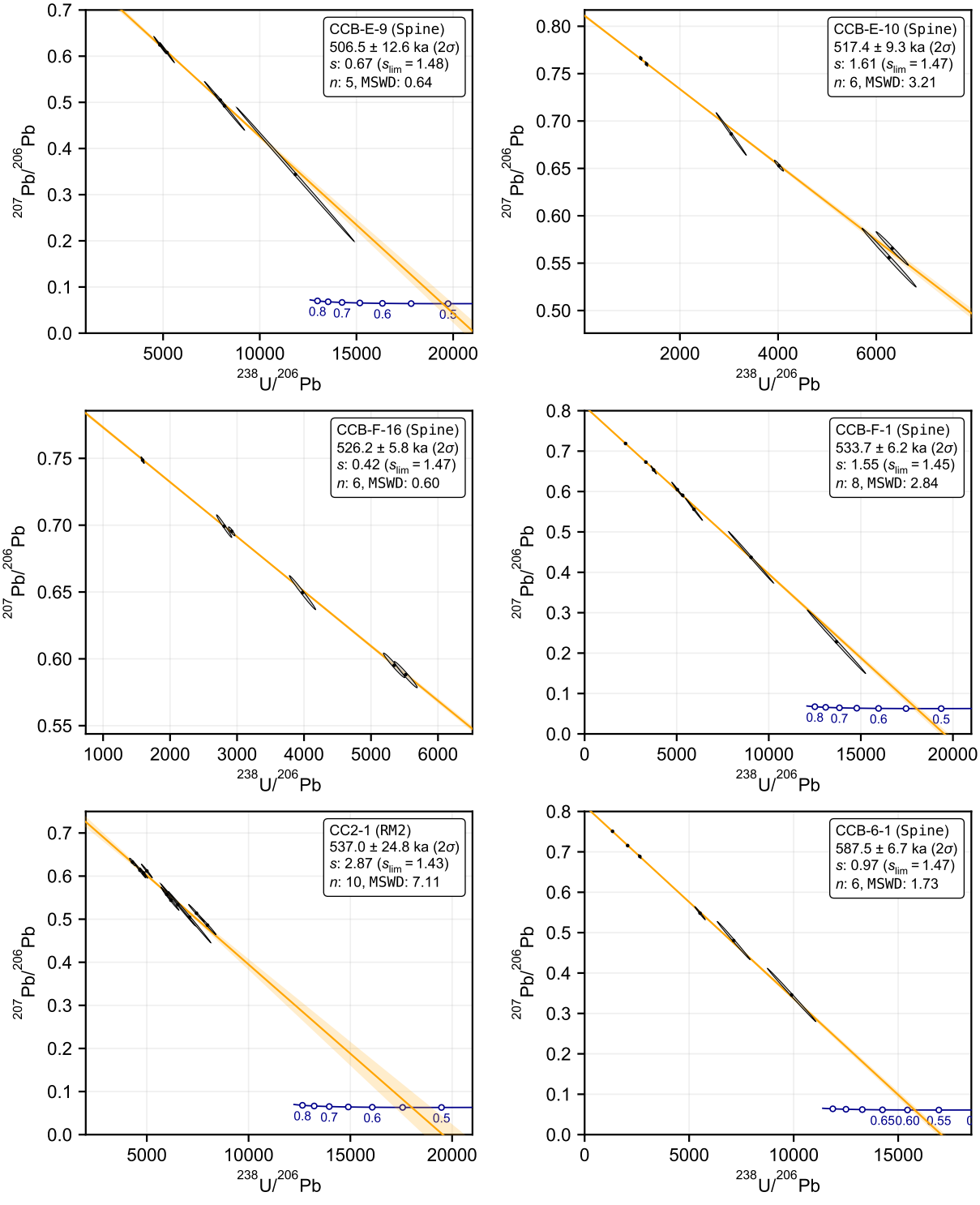

https://doi.org/10.5194/egusphere-2024-3594
Preprint. Discussion started: 22 November 2024

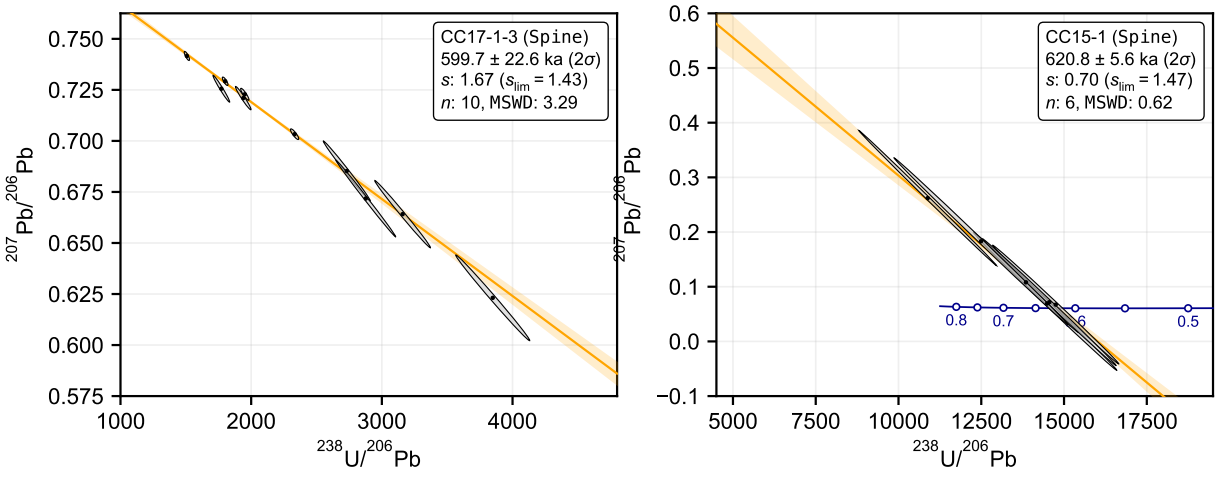

Figure 2. U–Pb Tera-Wasserburg isochron diagrams. Measured data points are plotted as 95% confidence ellipses (grey) along with the fitted isochron lines (orange) and their 95% confidence bands. The dark blue line shows the disequilibrium concordia curve, constructed using the measured $[^{234}U/^{238}U]$ value and assuming $[^{230}Th/^{238}U] = [^{226}Ra/^{238}U] = [^{231}Pa/^{235}U] = 0$. The disequilibrium concordia is truncated at the youngest age point associated with a physically impossible negative initial activity ratio solution following McLean et al. (2016). Shown in the textboxes is the spine width, s, value for a `spine` regression fit and simulated upper 95% confidence limit on s (see text for further discussion). The `MSWD` for a classical weighted least-squares regression (e.g. York et al., 2004) is also provided for comparison with other data sets. The regression model implemented is indicated in brackets: `spine` indicates use of the algorithm described by Powell et al. (2020), `RM2` indicates use of the Robust Model 2 algorithm (Pollard et al., 2023).

U–Pb ages, and thus uncertainty on the age difference was calculated simply by first-order analytical error propagation. A formal p-value under the null hypothesis that there is no significant age difference was then obtained from the standard normal CDF (see Table 1). For older U–Th ages (i.e. samples CCB-6-1, CC17-1-3, and CC15-1), however, U–Th age uncertainty distributions were positively skewed, and therefore, for these samples, the assumption that uncertainty in the age difference conforms to a strict Gaussian distribution is somewhat inaccurate (e.g. Ludwig, 2003). In these cases, we instead implemented a Monte Carlo procedure to simulate the age difference distribution (see The Supplement for details). Analogous to the formal hypothesis test, we concluded that the age difference was consistent with zero if the estimated 95% confidence interval on the Monte Carlo simulated age difference overlapped zero. Because analytical uncertainties on each pair of ages depends on a common measured $[^{234}U/^{238}U]$ value, age uncertainties are positively correlated, and this has the effect of reducing uncertainty on the age difference somewhat. We accounted for this effect by estimating U–Th versus U–Pb age correlation coefficients via Monte Carlo simulation and included this in the age difference uncertainty calculation. However, we note that the effect was minor in all cases (correlation coefficients were all less than 0.14 and averaged 0.05) and negligible where U–Pb regression-fitting uncertainties were relatively large.

https://doi.org/10.5194/egusphere-2024-3594
Preprint. Discussion started: 22 November 2024

U–Th and U–Pb ages for all samples were found to be consistent within analytical uncertainties (Fig. 3) except for sample CCB-6-1, where the U–Th age was significantly older than the U–Pb age (by 41 $+34/-25$ ka, 95% confidence level). In this instance, we consider the U–Pb age to be more reliable for two reasons. Firstly, the U–Pb isochron is well-behaved, with good spread in U/Pb ratios along the isochron and data point scatter about the isochron that is consistent with analytical uncertainties ($s < s_{\mathrm{lim}}$ and $p = 0.14$ for a classical least-squares fit). Secondly, the U–Pb age is more consistent with the stratigraphic position of the sample when age determinations for all three stalagmites are aligned to a common depth scale by synchronising their carbon (δ^{13}C) and oxygen (δ^{18}O) stable isotope profiles—noting that there is generally very good agreement between isotopic variations amongst coeval speleothems from Galleria delle Stalattiti (e.g. Bajo et al., 2020). The cause of the slightly older-than-expected U–Th age in this case is unclear, but one possibility is that this particular sub-sample was affected by localised open-system behaviour which resulted in post-depositional U loss and thus an older-than-true U–Th age determination. This is known to affect some speleothem samples even if they visually appear pristine (Bajo et al., 2016).

We also tested consistency between the age determinations on a collective basis. If the two chronometers are consistent and unbiased, the ages would be expected to plot along a 1:1 line that passes through the origin within their uncertainties. We plotted the U–Th age of each sample against its corresponding U–Pb age (excluding sample CCB-6-1, which was already found to be inconsistent on a pairwise basis) and fitted a regression line through the data, using an algorithm that accounts for uncertainty in both variables and uncertainty correlations (York et al., 2004) (Fig. 3). The best-fit regression line had a slope of 0.98 ± 0.07 (95% CI), y-intercept of 6.4 ± 31 (95% CI), and MSWD value of 0.52 (n=14, p=0.72), indicating that the paired ages are consistent with a 1:1 line within analytical uncertainties. We also assessed goodness-of-fit of the paired ages to a 1:1 line directly, obtaining an MSWD of 0.95 (n=14, p=0.49). These results suggest that the two chronometers are consistent and unbiased over the age interval considered.

One limitation of this approach, however, is that, as noted above, the U–Th age analytical uncertainties for older samples CC15- 1 and CC17-1-3 are slightly non-Gaussian, leading to some inaccuracy in regression results obtained by the classical least-squares approach, which assumes strictly Gaussian uncertainty distributions. Nevertheless, these samples have relatively large age uncertainties that comfortably overlap the best-fit line, and thus we consider the results to be relatively insensitive to this assumption.

4.2 Age precision

The nature of final age uncertainties differs considerably between the two chronometers. The magnitude of U–Th age uncertainties are more predictable than U–Pb age uncertainties, and generally increase in an approximately exponential manner with age, from ~4.5 ka (2σ) at ~450 ka to >25 ka (2σ) at ~620 ka. When U–Th age uncertainties are plotted against age, the data lie close to a prediction based on age uncertainty propagation using average [^{234}U/^{238}U] and [^{230}Th/^{238}U] measurement uncertainties for samples in this study (Fig. 5). Scatter about this prediction line generally correlates with uncertainty on measured [^{234}U/^{238}U] and [^{230}Th/^{238}U] values. From a broader perspective, U–Th age uncertainties are expected to also depend some-

https://doi.org/10.5194/egusphere-2024-3594
Preprint. Discussion started: 22 November 2024

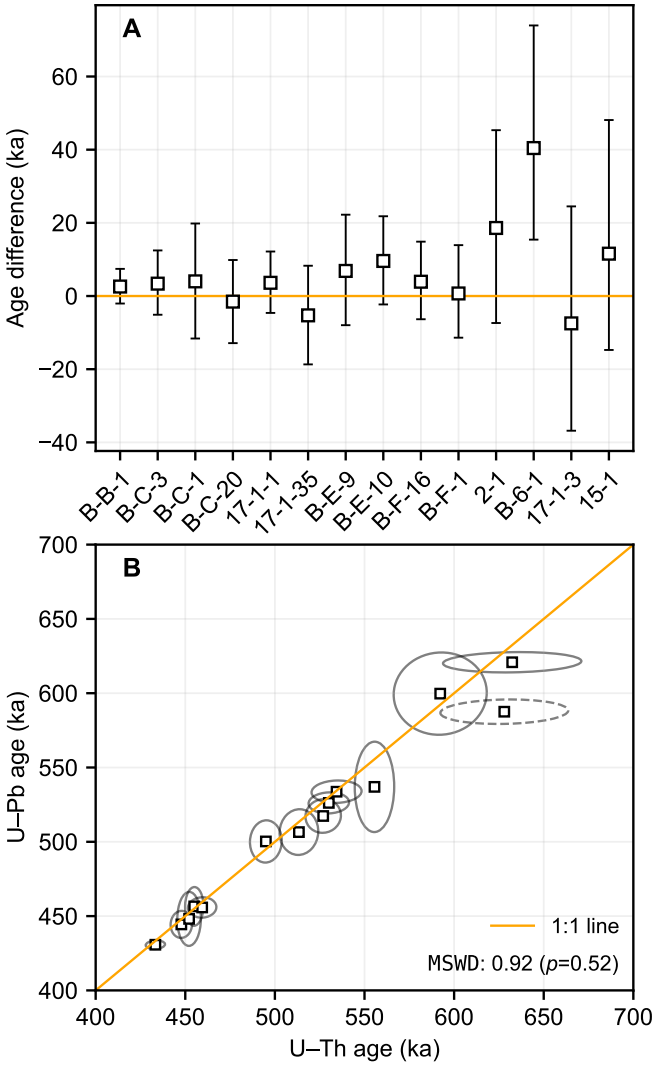

Figure 3. Comparison of U–Th and U–Pb age determinations. (**A**) Age difference for each sample calculated as: $U\text{-}Th\ age - U\text{-}Pb\ age$. Note that the 'CC' prefix of each sample ID has been omitted. (**B**) Collective comparison U–Th and U–Pb ages. The confidence ellipse for sample CCB-6-1, which was found to be inconsistent on a pairwise basis and therefore excluded from the `MSWD` calculation, is plotted with the dashed outline. Error bars and confidence ellipses are plotted at the 95% confidence level.

what on $[^{234}U/^{238}U]_i$ (where subscript i denotes an initial activity ratio), with smaller uncertainties generally accompanying higher $[^{234}U/^{238}U]_i$ values for samples of the same age (e.g Meckler et al., 2012). However, owing to the limited $[^{234}U/^{238}U]_i$ variability of the samples analysed in this study, this effect on U–Th age precision could not be assessed here. Nevertheless, we note that the low $[^{234}U/^{238}U]_i$ values of Corchia speleothems may lead to slightly lower U–Th age precision than could be obtained in otherwise identical carbonates with higher $[^{234}U/^{238}U]_i$.

https://doi.org/10.5194/egusphere-2024-3594
Preprint. Discussion started: 22 November 2024

Table 2. Summary of pairwise U–Th versus U–Pb age comparison

Sample ID	Age (ka)[1]	Age diff. (ka)[2]	Age diff. 95% CI (ka)[4]	p-value[5]	Significant difference?[6]
CCB-B-1	431.3	2.6	(-2.03, 7.42)	0.27	no
CCB-C-3	446.8	3.4	(-5.11, 12.46)	0.44	no
CCB-C-1	451.7	4.0	(-11.61, 19.82)	0.61	no
CCB-C-20	455.2	-1.5	(-12.87, 9.8)	0.79	no
CC17-1-1	457.4	3.6	(-4.6, 12.2)	0.39	no
CC17-1-35	496.4	-5.3	(-18.7, 8.3)	0.43	no
CCB-E-9	511.1	6.9	(-8.0, 22.2)	0.36	no
CCB-E-10	522.8	9.6	(-2.3, 21.8)	0.11	no
CCB-F-16	527.3	3.9	(-6.3, 14.9)	0.46	no
CCB-F-1	533.9	0.7	(-11.4, 13.9)	0.91	no
CC2-1	553.4	18.6	(-7.4, 45.3)	0.16	no
CCB-6-1	589.6	40.4	(15.4, 74.0)	0.01*	yes
CC17-1-3	595.6	-7.5	(-36.8, 24.5)	0.62 *	no
CC15-1	621.2	11.6	(-14.7, 48.1)	0.46*	no

[1]Weighted average of U–Th and U–Pb ages. [2]Age difference calculated as: U–Th age − U–Pb age. [3]Assuming Guassian distributed analytical uncertainties. [4]Based on Monte Carlo simulation. [5]p-value under the null hypothesis that there is no significant age difference. [6] Result of the hypothesis test of age consistency ($\alpha = 0.05$ level of significance). *p-value should be interpreted as a qualitative indicator only (see text).

U–Pb age uncertainties, on the other hand, do not show an obvious trend with increasing age and do not correlate directly with average analytical uncertainties on $^{206}Pb/^{207}Pb$ or $^{238}U/^{206}Pb$ isotope ratio measurements. Moreover, there is minimal correlation between U–Pb age uncertainties in this dataset and [$^{234}U/^{238}U$] measurement precision, or scatter of data about the isochron (quantified either by the `MSWD` statistic, or its robust variant, s). Instead, U–Pb age uncertainties appear to depend predominantly on the distribution of data along the isochron, consistent with the findings of previous studies (Woodhead and Pickering, 2012; Engel and Pickering, 2022).

Engel and Pickering (2022) examined factors controlling U–Pb isochron age precision in Middle Pleistocene speleothems from multiple cave sites, including Corchia Cave. They found that uncertainty in Tera-Wasserburg U–Pb isochron ages generally correlates strongly with uncertainty in the isochron regression slope, which is in-turn controlled largely by spread in Pb/U ratios of data along the isochron line due to variability in inherited-Pb content. To quantify the spread of data points along the isochron, Engel and Pickering (2022) defined a metric termed 'average isochron distance', which quantifies the spread of data as the average Euclidean distance between each data point and the centroid of the data set ($\bar{x}$, $\bar{y}$). Here we adopt an alternative

https://doi.org/10.5194/egusphere-2024-3594
Preprint. Discussion started: 22 November 2024

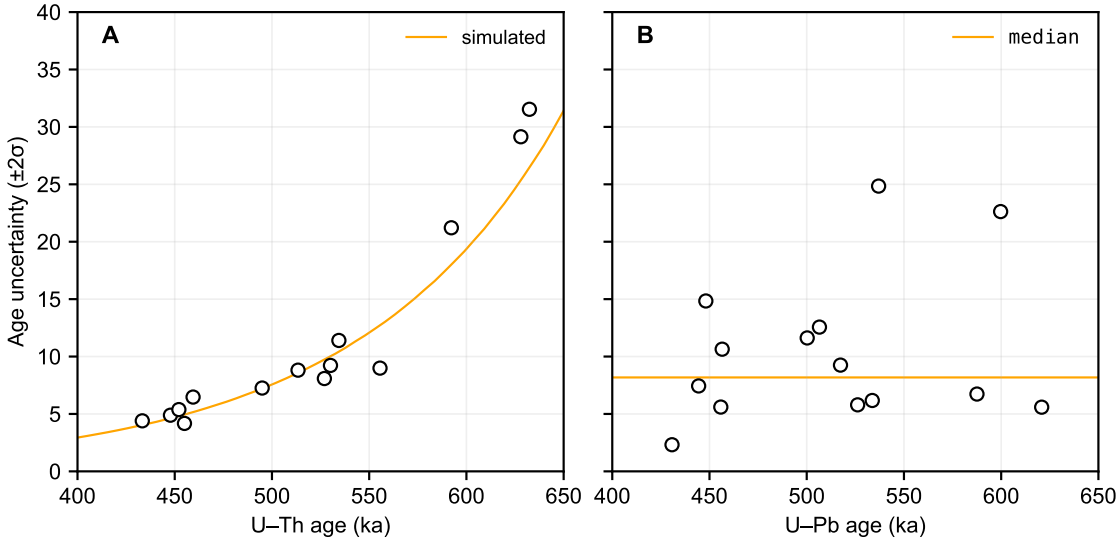

Figure 4. Age precision versus age for U–Th and U–Pb age determinations The orange line in (**A**) shows the predicted U–Th age uncertainty calculated using Monte Carlo simulation and based on the average [^{234}U/^{238}U] and [^{230}Th/^{238}U] measurement uncertainties for samples analysed in this study and an assumed [^{234}U/^{238}U]$_i$ value of 0.72, which is typical of Corchia Cave stalagmites in this age range. The orange line in (**B**) shows the median U–Pb age uncertainty over this interval.

metric based on the least-squares fitted points[1] along the regression line (York et al., 2004) rather than the measured data points themselves. In this context, use of the least-squares fitted points helps to better differentiate between spread of data *along* the isochron and scatter *about* the isochron (e.g. due to 'geological' scatter). It also circumvents scaling issues associated with isochron diagram axes spanning vastly different orders of magnitude, as is the case for the Tera-Wasserburg diagram. The metric we adopt is termed 'combined isochron spread' and calculated as

$$d_x = \sqrt{\sum_k (x_k - \bar{x})^2} \tag{1}$$

where x_k is the least-squares fitted ^{238}U/^{206}Pb value of the k^{th} data point and $\bar{x}$ is the centroid of the data points.

In addition to spread of data points along the isochron, another factor that influences Tera-Wasserburg isochron age uncertainties is the location of the data relative to the concordia intercept point. Uncertainty in an isochron regression line may be visualised as a hyperbolic confidence band with a minimum width near to, or precisely at (in the case of the least-squares regression, e.g. York et al. (2004)), the data centroid ($\bar{x}$, $\bar{y}$) (e.g. Ludwig, 1980). Therefore, uncertainty bounds on a concordia intercept age tend to increase as the data centroid moves further away from the intercept point. To assess this effect on U–Pb

[1]The least-squares fitted points (or 'least-squared adjusted' points, York et al., 2004) are the points along the regression line with the highest probability of generating the 'uncertainty perturbed' measured data points assuming that assigned analytical uncertainties are the only reason for the measurements to depart from the isochron line.

https://doi.org/10.5194/egusphere-2024-3594
Preprint. Discussion started: 22 November 2024

isochron age uncertainties, we define a second metric termed the 'average inherited Pb index', which is calculated as:

$$\bar{Pb}_i = \frac{\bar{y} - y^*}{y_0 - y^*} \quad (2)$$

where y^* is the $^{207}Pb/^{206}Pb$ value of the concordia intercept point, $\bar{y}$ is the centroid of the data, and y_0 is the y-axis intercept point (i.e. the estimated $^{207}Pb/^{206}Pb$ value from the regression fit). Essentially, this is the distance in y between the concordia intercept point and the centroid of the data, normalised to the maximum possible spread of data in along an isochron of given age, initial $^{207}Pb/^{206}Pb$ isotopic composition, and initial $[^{234}U/^{238}U]$ value.

Consistent with Engel and Pickering (2022), we find that the spread of data along the isochron line is controlled by variations in inherited-Pb content rather than U content, with the latter tending to remain relatively constant across speleothem growth layers (see The Supplement). Moreover, because there is an inverse relationship between isochron data spread and total Pb content, greater variation in inherited Pb content is required to achieve a given level of data spread along the isochron (and thus a given slope uncertainty) for less radiogenic datasets. We find that U–Pb isochron age uncertainties correlate strongly with uncertainty in the isochron slope, excluding the highly radiogenic (i.e. very low inherited Pb) samples CC15-1 and CCB-C-3, which encompass multiple data points plotting close to, or overlapping, the disequilibrium concordia curve (Fig. 5a). In turn, isochron slope precision correlates somewhat with the combined isochron spread (Fig. 5b), although sample CCB-C-20, which has an exceptionally low dispersion of data about the regression line (MSWD = 0.15), clearly does not conform to this general trend.

Overall, we find that U–Pb isochron ages of similar average precision can be obtained throughout the ca. 430–630 ka interval considered in this study provided that the isochron either encompasses data points with a reasonable spread in Pb/U ratios or includes highly radiogenic material. In practical terms, there are a number of ways in which samples can be pre-screened for suitability in this regard. A number of options were discussed in Woodhead et al. (2012) but advances in both chemical separation procedures (allowing rapid sample throughput) and the development of in situ analytical techniques (e.g. Roberts et al., 2020) have now rendered some of these approaches redundant. Currently, the most accurate and time-efficient methods for assessing suitability for U–Pb dating would appear to be either pre-screening via laser ablation ICP-MS (e.g. Woodhead and Petrus, 2019), U–Th isotopic analysis using a high-throughput protocol (e.g. Hellstrom, 2003) whereby ^{232}Th is employed as a proxy for inherited Pb (Woodhead et al., 2006), or simple reconnaissance ID analysis involving a small number (~ 3) of sub-samples taken from different parts of the growth domain.

4.2.1 Relative age precision

Average U–Pb isochron age uncertainties may be reasonably quantified either as the mean, ± 10.4 ka (2σ), or median, ± 8.3 ka (2σ) age uncertainty, although in this context we believe that the median offers a more useful indicator of average expected age uncertainty because it down-weights the influence of isochrons CC2-1 and CC17-1-3, which have anomalous age uncertainties compared to the other samples. In our dataset, average predicted U–Th age uncertainties exceed median U–Pb age uncertainties

https://doi.org/10.5194/egusphere-2024-3594
Preprint. Discussion started: 22 November 2024

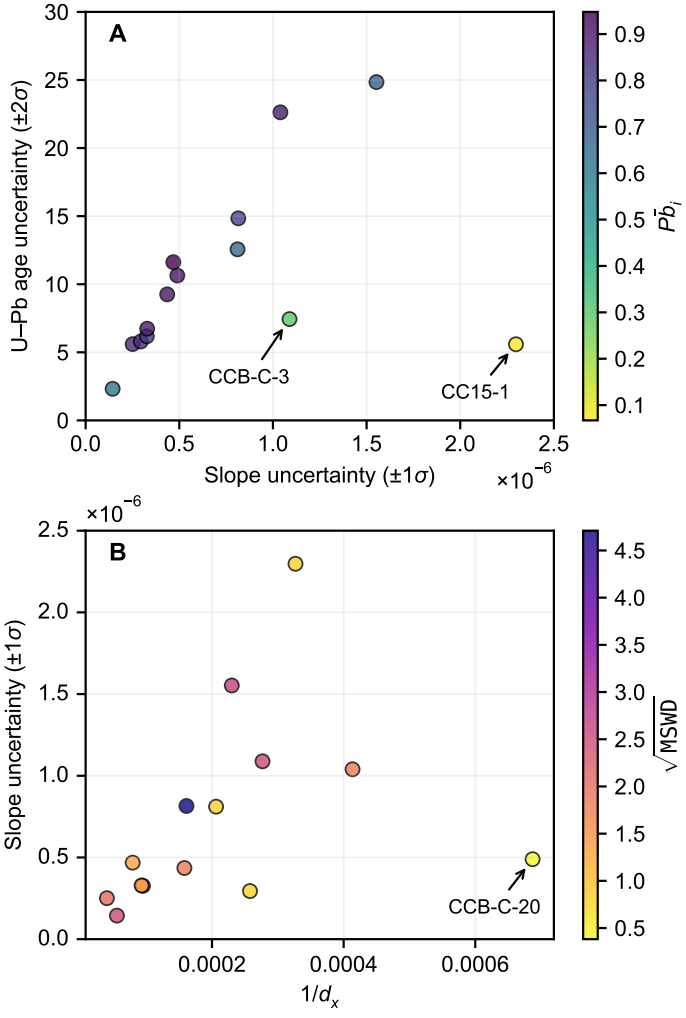

Figure 5. Factors controlling U–Pb isochron age precision. (**A**) U–Pb age uncertainty plotted against uncertainty in the isochron slope. Markers are coloured according to $\bar{P}b_i$ (i.e. the 'inherited Pb index', Eq. 2). Age uncertainty generally correlates strongly with uncertainty on the isochron slope, except where isochrons are highly radiogenic (i.e. have very low average inherited Pb). (**B**) Isochron slope uncertainty plotted against the reciprocal of the 'combined isochron spread' (d_x) metric (Eq. 1). Generally speaking, isochron slope uncertainty is correlated with the inverse of combined Pb/U spread. An obvious exception is sample CCB-C-20, which exhibits very little data scatter about the isochron. Markers are coloured according to $\sqrt{\text{MSWD}}$, employed here as an indicator of data dispersion about the isochron.

at ~520 ka (Fig. 4), suggesting that U–Pb dating may generally provide higher precision ages beyond this point. However, there are two important caveats to this finding. Firstly, the exact overlap point is expected to vary considerably across different cohorts of samples and depend on various sample characteristics. For example, speleothems from Corchia Cave have relatively high U and very low average inherited-Pb content, making them very well-suited to U–Pb geochronology (Woodhead et al.,

https://doi.org/10.5194/egusphere-2024-3594
Preprint. Discussion started: 22 November 2024

2006). At the same time, the initial [^{234}U/^{238}U] values of these samples, which are all significantly below unity, limits precision of the U–Th dating method relative to other study sites and samples with similar U and initial Th content, but higher initial [^{234}U/^{238}U]. Therefore, the age precision overlap point would be expected to be somewhat higher for other study sites and samples. Secondly, from a practical point of view, U–Pb isochron ages are significantly more labour intensive on a per-age basis compared to U–Th ages given that they require analysis of several coeval sub-samples (typically >4). Thus, in applications where multiple age determinations are combined so that final age uncertainties are a product of multiple U–Th and/or U–Pb age determinations, e.g. in compiling a depth-age model along the axial length of a speleothem (e.g. Scholz et al., 2012; Bajo et al., 2012), the U–Th chronometer may still deliver lower final depth-age model uncertainties for a given number of analyses beyond this age precision overlap point.

4.3 ^{238}U/^{235}U values

Variations in ^{238}U/^{235}U ratios are relatively minor in nature and, until recently, could not be resolved using routine measurement protocols. For this reason, ^{238}U/^{235}U has traditionally been treated as a constant in geochronology, with a 'consensus value' of 137.88 (Steiger and Jäger, 1977) ubiquitously adopted. However, the development of high precision ^{238}U/^{235}U measurement protocols over the past two decades have revealed variations in natural ^{238}U/^{235}U ratios (typically expressed as δ^{238}U values) of up to a few ‰ (e.g. Stirling et al., 2007; Weyer et al., 2008; Tissot and Dauphas, 2015). These variations are attributed predominately to U fractionation associated with nuclear volume effects rather than classical mass-dependent fractionation (Fujii et al., 2009) and appear to be most significant during redox reactions. Notably, during the reduction of soluble U^{6+} to insoluble U^{4+}, ^{238}U is concentrated in the U^{4+} state, leaving the insoluble phase with a higher ^{238}U/^{235}U than the remaining dissolved U. This forms the basis of efforts to employ δ^{238}U values of marine sediments as a palaeoredox proxy (e.g. Andersen et al., 2014). Processes such as adsorption (e.g. Weyer et al., 2008) and mineral leaching by strong acids (Stirling et al., 2007; Hiess et al., 2012) have also been observed to induce ^{238}U/^{235}U fractionation, while oxidation of U is not associated with significant fractionation.

Analyses conducted over the past ∼15 years suggest that the average δ^{238}U of bulk crustal rocks (δ^{238}U=∼-0.29 ‰) is practically indistinguishable from that of the deep mantle (δ^{238}U=∼-0.31) (Andersen et al., 2017; Tissot and Dauphas, 2015). The upper mantle is somewhat more enriched in ^{238}U on average due to recycling of altered oceanic crust (Andersen et al., 2015), whereas modern ocean water and marine carbonates are more depleted in ^{238}U (∼-0.39 ‰ Tissot and Dauphas, 2015). Accessory U minerals show more δ^{238}U variability than bulk crustal rocks, as do materials formed in low-temperature environments (Stirling et al., 2007; Weyer et al., 2008; Hiess et al., 2012). To date, only a small number of studies have reported δ^{238}U values for speleothems. For example, Stirling et al. (2007) and Cheng et al. (2013) presented δ^{238}U values for speleothems from numerous cave systems and observed highly variable δ^{238}U values (ranging from ∼-0.7 to +0.4 ‰), although variability within a single speleothem or cave system was significantly lower (Shen et al., 2012). Stirling et al. (2007) also identified a tentative correlation between speleothem δ^{238}U and measured [^{234}U/^{238}U] values, suggesting that speleothem ^{234}U-disequilibrium and ^{238}U/^{235}U fractionation may be linked via a common weathering control, albeit involving different fractionation mechanisms.

https://doi.org/10.5194/egusphere-2024-3594
Preprint. Discussion started: 22 November 2024

The use of a high precision all-Faraday-cup protocol for U–Th measurements in this study, which employs a ^{233}U-^{236}U double spike for mass bias correction, permits measurement of accurate and precise ^{238}U/^{235}U values. Average analytical uncertainty in measured ^{238}U/^{235}U ratios were 0.0006 (2σ), which is adequate for assessing δ^{238}U variability at the sub-‰ level (see Table 1). We compared the speleothem δ^{238}U data obtained in this study with data presented in previous studies (Fig. 6). This preliminary compilation suggests that most speleothem δ^{238}U values lie within a range from approximately -0.6 to -0.2 ‰, consistent with the range observed for carbonate rocks globally (Li and Tissot, 2023). The majority of these data are therefore not inconsistent with the simple hypothesis that speleothems acquire their ^{238}U/^{235}U isotopic composition from the carbonate host rock in the absence of significant U-isotope fractionation. However, two of the Nullarbor speleothem samples (MO-1/3) and the KOZ samples are significantly more enriched in ^{238}U than carbonate rocks, suggesting either a more ^{238}U-enriched non-carbonate source of U or the presence of an enriching fractionation process during source water U uptake and/or transport to the site of speleothem deposition. Clearly further studies are required to investigate the cause of these high δ^{238}U values, as well as the primary controls on speleothem δ^{238}U values more generally.

We also compared the δ^{238}U and measured [^{234}U/^{238}U] values of the speleothem data obtained in this study with data from previous studies to further assess the relationship between speleothem ^{234}U-disequilibrium and ^{238}U/^{235}U fractionation (see The Supplement). With the inclusion of additional speleothem data from this study and others, we observed a weaker correlation ($R^2 = 0.42$) between δ^{238}U and measured [^{234}U/^{238}U] values than Stirling et al (2007), and this correlation becomes negligible if the 'high leverage' KOZ data are excluded. However, for speleothem samples that are presumed to have acted as a closed system with respect to U-series isotopes post deposition, it is arguably more appropriate to compare δ^{238}U values with initial [^{234}U/^{238}U] values instead of measured activity ratios, since measured [^{234}U/^{238}U] values also depend on sample age. When repeating this comparison using initial [^{234}U/^{238}U] values instead of measured values (necessarily excluding a number of samples for which no age data was available), no correlation is observed ($R^2 = 0.01$). This result is inconsistent with the hypothesis that speleothem ^{234}U-disequilibrium and ^{238}U/^{235}U fractionation are linked by a common weathering control.

Regardless of the dominant controls on speleothem δ^{238}U values, the data available thus far show that the U isotopic composition of most speleothems departs significantly from the conventional ^{238}U/^{235}U value of (Steiger and Jäger, 1977), and also to a lesser extent, the average terrestrial zircon value of Hiess et al. (2012). Using a present-day ^{238}U/^{235}U value of ~137.79 (the weighted average obtained for speleothem samples in this study) in place of the traditional value of 137.88 (Steiger and Jäger, 1977), either for mass bias correction of U–Pb data and/or in U–Pb age calculation, has a negligible effect on U–Pb ages for young (e.g. Cenozoic) samples. However, when applying the Pb/Pb dating approach to older materials, the ^{238}U/^{235}U value adopted can have a significant effect on age accuracy (Stirling et al., 2007; Weyer et al., 2008; Hiess et al., 2012). This is also the case in U–Th dating using an assumed ^{238}U/^{235}U value either for mass bias correction or calculating ^{238}U-based ratios from measured ^{235}U (Stirling et al. 2007, Cheng et al. 2013), although the magnitude of the inaccuracy depends greatly on the specific analytical protocol that is adopted (Shen et al., 2012). The significant departure of speleothem ^{238}U/^{235}U values from

https://doi.org/10.5194/egusphere-2024-3594
Preprint. Discussion started: 22 November 2024

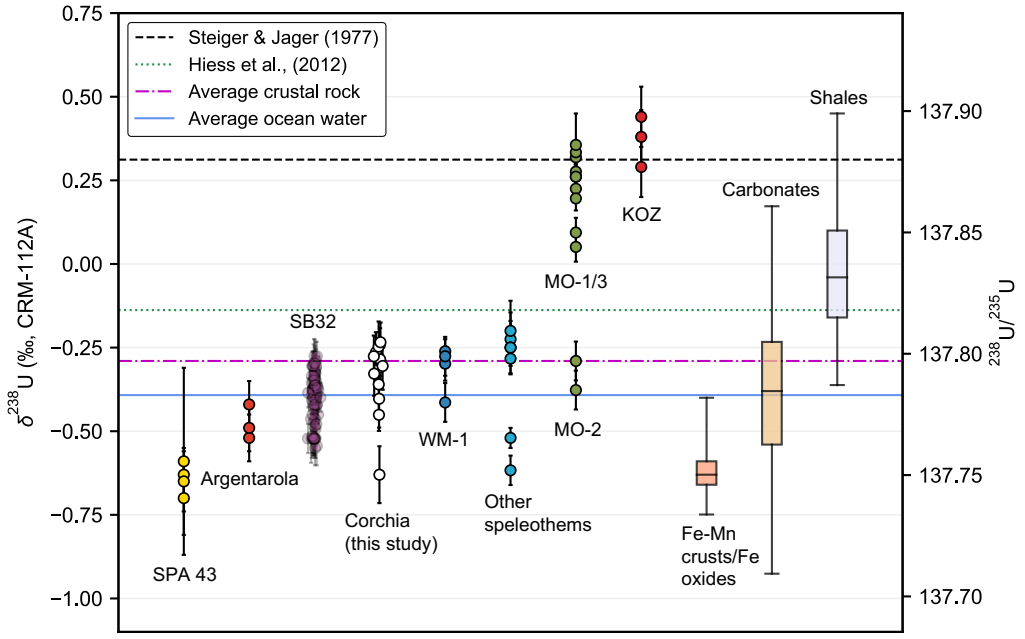

Figure 6. Compilation speleothem δ^{238}U data from this study and others. Speleothem samples are grouped according to cave site where more than two analyses were available. Speleothem data from Cheng et al., (2013) include SB32 from Sanbao Cave, central China (e.g. Wang et al., 2008), WM1 from Wilder Mann Cave, Northern Calcareous Alps, Austria (Meyer et al., 2009), and MO-1/2/3 from Leana's Breath Cave, Nullarbor Plain, Australia (Woodhead et al., 2006). 'Other speleothems' includes the GBW04412 and GBW04413 stalagmite standards from Wang et al. (2023), the FAB-LIG Sample from Stirling et al., (2007), and the Kr3 and CA-1 samples from Cheng et al., (2013). Speleothem samples analysed by Stirling et al. (2007) include SPA-43 from Spannegal Cave, Austria (e.g. Spötl and Mangini, 2010), Argentaorola from Argentarola Island, central Italy (e.g. Bard et al., 2002), and KOZ. Also shown are the 'consensus' ^{238}U/^{235}U value of Steiger and Jäger (1977), the average terrestrial zircon value of Hiess et al., (2012), and the average modern ocean water (–0.39 ‰) and crustal rock (–0.29 ‰) values (Tissot and Dauphas, 2015). The global range of δ^{238}U values for carbonates, Phanerozoic shales, and Fe-Mn crusts/Fe oxides are also shown as box plots based on data compiled by Li et al. (2023), with 'whiskers' indicating the 2.5 and 97.5 percentiles. Absolute ^{238}U/^{235}U values are shown on the right-hand y-axis based on the ^{238}U/^{235}U$_{\mathrm{CRM\text{-}112A}}$ value of 137.837 from Richter et al. (2010).

137.88 that is observed here re-iterates the need to pay careful attention to the ^{238}U/^{235}U value used when dating carbonates under these circumstances.

5 Conclusions

This comparison of the carbonate U–Th and U–Pb chronometers demonstrates excellent agreement between the two dating methods over a substantial part of the Middle Pleistocene. In comparing the performance of the two chronometers, we find that U–Th age uncertainties are much more predictable than U–Pb isochron age uncertainties and tend to increase in an

https://doi.org/10.5194/egusphere-2024-3594
Preprint. Discussion started: 22 November 2024

approximately exponential manner over the ca. 430–630 ka age interval considered. On the other hand, U–Pb age uncertainties do not increase in a systematic manner but are highly dependent on uncertainty in the isochron slope, which is in turn largely controlled by the U/Pb spread of data points along the isochron, and the availability of highly radiogenic (i.e. low inherited Pb) material. Furthermore, we find that the U–Pb method (via ID MC-ICP-MS) is capable of achieving precision surpassing that of the U–Th method prior to the latter reaching its upper age limit. For our dataset, the average precision of U–Pb ages exceeds that of U–Th ages at ∼520 ka, although the exact overlap point is expected to vary across different sample types and study sites. However, even where U–Pb isochron age precision clearly surpasses that of U–Th age determinations, the U–Th chronometer may still offer practical advantages, especially when combining multiple age determinations (e.g. in compiling speleothem depth-age models), because it is less labour intensive on a per-age basis. Taken as a whole, these findings suggest that both the U–Th and U–Pb methods will continue to play an important role in developing accurate and precise chronologies for Middle Pleistocene carbonates, and support the prospect of compiling internally consistent U-series based chronologies throughout the Middle Pleistocene and beyond. Finally, in line with previous studies, we find that speleothem $^{238}U/^{235}U$ values are often significantly lower than the nominal value of 137.88 (Steiger and Jäger, 1977), which has traditionally been adopted as a constant in geochronology. This re-emphasises the need to pay careful attention to the $^{238}U/^{235}U$ value used for data processing and age calculation in cases where it exerts a significant impact on calculated U–series or Pb/Pb ages.

Data availability. All data used for age calculations and subsequent statistical analyses are available in The Supplement.

Author contributions. GZ, RD, II, JH, ER, and TP collected the samples, and undertook preliminary analyses to identify those suitable for this study. RLE, HC, MP, and XL, developed the U–Th analytical protocol, and TP, MP, XL, and DP carried out the U–Th analyses. TP, JW, and AW carried out the U–Pb analyses. TP undertook the statistical analyses and wrote the manuscript with contributions from all co-authors.

Competing interests. The authors declare that they have no competing interests.

Acknowledgements. We are grateful to the Gruppo Speleologico Lucchese for their assistance with the recovery of speleothem samples used in this study. We thank Cameron Patrick of the Statistical Consulting Centre, University of Melbourne, for advice on certain aspects of the age comparison. This research was funded by Australian Research Council Discovery Project grants DP160202969 (to RD, JW, JH, ER and GZ), DP220102133 (to RD, JW, and ER), and FL160100028 to JW..

https://doi.org/10.5194/egusphere-2024-3594
Preprint. Discussion started: 22 November 2024

References

Andersen, M. B., Stirling, C. H., Potter, E.-K., and Halliday, A. N.: Toward epsilon levels of measurement precision on $^{234}U/^{238}U$ by using MC-ICPMS, International Journal of Mass Spectrometry, 237, 107–118, https://doi.org/10.1016/j.ijms.2004.07.004, 2004.

Andersen, M. B., Romaniello, S., Vance, D., Little, S. H., Herdman, R., and Lyons, T. W.: A modern framework for the interpretation of $^{238}U/^{235}U$ in studies of ancient ocean redox, Earth and Planetary Science Letters, 400, 184–194, https://doi.org/10.1016/j.epsl.2014.05.051, 2014.

Andersen, M. B., Elliott, T., Freymuth, H., Sims, K. W. W., Niu, Y., and Kelley, K. A.: The terrestrial uranium isotope cycle, Nature, 517, 356–359, https://doi.org/10.1038/nature14062, 2015.

Andersen, M. B., Stirling, C. H., and Weyer, S.: Uranium isotope fractionation, Reviews in Mineralogy and Geochemistry, 82, 799–850, https://doi.org/10.2138/rmg.2017.82.19, 2017.

Bajo, P., Drysdale, R., Woodhead, J., Hellstrom, J., and Zanchetta, G.: High-resolution U–Pb dating of an early pleistocene stalagmite from corchia cave (central italy), Quaternary Geochronology, 14, 5–17, https://doi.org/10.1016/j.quageo.2012.10.005, 2012.

Bajo, P., Hellstrom, J., Frisia, S., Drysdale, R., Black, J., Woodhead, J., Borsato, A., Zanchetta, G., Wallace, M. W., Regattieri, E., and Haese, R.: "Cryptic" diagenesis and its implications for speleothem geochronologies, Quaternary Science Reviews, 148, 17–28, https://doi.org/10.1016/j.quascirev.2016.06.020, 2016.

Bajo, P., Borsato, A., Drysdale, R., Hua, Q., Frisia, S., Zanchetta, G., Hellstrom, J., and Woodhead, J.: Stalagmite carbon isotopes and dead carbon proportion (DCP) in a near-closed-system situation: An interplay between sulphuric and carbonic acid dissolution, Geochimica et Cosmochimica Acta, 210, 208–227, https://doi.org/10.1016/j.gca.2017.04.038, 2017.

Bajo, P., Drysdale, R. N., Woodhead, J. D., Hellstrom, J. C., Hodell, D., Ferretti, P., Voelker, A. H. L., Zanchetta, G., Rodrigues, T., Wolff, E., Tyler, J., Frisia, S., Spötl, C., and Fallick, A. E.: Persistent influence of obliquity on ice age terminations since the Middle Pleistocene transition, Science, 367, 1235–1239, https://doi.org/10.1126/science.aaw1114, 2020.

Bard, E., Delaygue, G., Rostek, F., Antonioli, F., Silenzi, S., and Schrag, D. P.: Hydrological conditions over the western Mediterranean basin during the deposition of the cold Sapropel 6 (ca. 175 kyr BP), Earth and Planetary Science Letters, 202, 481–494, https://doi.org/10.1016/S0012-821X(02)00788-4, 2002.

Barlow, R. J.: A Guide to the Use of Statistical Methods in the Physical Sciences, The Manchester Physics Series, John Wiley & Sons, Chilchester, UK, ISBN 0-471-92294-3, 1989.

Cheng, H., Lawrence Edwards, R., Shen, C.-C., Polyak, V. J., Asmerom, Y., Woodhead, J., Hellstrom, J., Wang, Y., Kong, X., Spötl, C., Wang, X., and Calvin Alexander, E.: Improvements in ^{230}Th dating, ^{230}Th and ^{234}U half-life values, and U–Th isotopic measurements by multi-collector inductively coupled plasma mass spectrometry, Earth and Planetary Science Letters, 371–372, 82–91, https://doi.org/10.1016/j.epsl.2013.04.006, 2013.

Cheng, H., Edwards, R. L., Sinha, A., Spötl, C., Yi, L., Chen, S., Kelly, M., Kathayat, G., Wang, X., Li, X., Kong, X., Wang, Y., Ning, Y., and Zhang, H.: The Asian monsoon over the past 640,000 years and ice age terminations, Nature, 534, 640–646, https://doi.org/10.1038/nature18591, 2016.

Cliff, R. A., Spötl, C., and Mangini, A.: U–Pb dating of speleothems from Spannagel Cave, Austrian Alps: A high resolution comparison with U-series ages, Quaternary Geochronology, 5, 452–458, https://doi.org/10.1016/j.quageo.2009.12.002, 2010.

https://doi.org/10.5194/egusphere-2024-3594
Preprint. Discussion started: 22 November 2024

Condon, D. J., Schoene, B., McLean, N. M., Bowring, S. A., and Parrish, R. R.: Metrology and traceability of U–Pb isotope dilution geochronology (EARTHTIME tracer calibration part I), Geochimica et Cosmochimica Acta, 164, 464–480, https://doi.org/10.1016/j.gca.2015.05.026, 2015.

Corrick, E. C., Drysdale, R. N., Hellstrom, J. C., Capron, E., Rasmussen, S. O., Zhang, X., Fleitmann, D., Couchoud, I., and Wolff, E.: Synchronous timing of abrupt climate changes during the last glacial period, Science, 369, 963–969, https://doi.org/10.1126/science.aay5538, 2020.

Denniston, R. F., Asmerom, Y., Polyak, V. Y., McNeill, D. F., Klaus, J. S., Cole, P., and Budd, A. F.: Caribbean chronostratigraphy refined with U-Pb dating of a Miocene coral, Geology, 36, 151–4, https://doi.org/10.1130/G24280A.1, 2008.

Drysdale, R., Couchoud, I., Zanchetta, G., Isola, I., Regattieri, E., Hellstrom, J., Govin, A., Tzedakis, P. C., Ireland, T., Corrick, E., Greig, A., Wong, H., Piccini, L., Holden, P., and Woodhead, J.: Magnesium in subaqueous speleothems as a potential palaeotemperature proxy, Nat Commun, 11, 5027, https://doi.org/10.1038/s41467-020-18083-7, 2020.

Drysdale, R. N., Zanchetta, G., Hellstrom, J. C., Fallick, A. E., Zhao, J.-x., Isola, I., and Bruschi, G.: Palaeoclimatic implications of the growth history and stable isotope δ^{18}O and δ^{13}C geochemistry of a Middle to Late Pleistocene stalagmite from central-western Italy, Earth and Planetary Science Letters, 227, 215–229, https://doi.org/10.1016/j.epsl.2004.09.010, 2004.

Drysdale, R. N., Hellstrom, J. C., Zanchetta, G., Fallick, A. E., Goñi, M. F. S., Couchoud, I., McDonald, J., Maas, R., Lohmann, G., and Isola, I.: Evidence for obliquity forcing of glacial termination II, Science, 325, 1527–1531, https://doi.org/10.1126/science.1170371, 2009.

Drysdale, R. N., Zanchetta, G., Baneschi, I., Guidi, M., Isola, I., Couchoud, I., Piccini, L., Greig, A., Wong, H., Woodhead, J. D., Regattieri, E., Corrick, E., Paul, B., Spötl, C., Denson, E., Gordon, J., Jaillet, S., Dux, F., and Hellstrom, J. C.: Partitioning of Mg, Sr, Ba and U into a subaqueous calcite speleothem, Geochimica et Cosmochimica Acta, 264, 67–91, https://doi.org/10.1016/j.gca.2019.08.001, 2019.

Edwards, R. L., Chen, J. H., and Wasserburg, G. J.: ^{238}U-^{234}U-^{230}Th-^{232}Th systematics and the precise measurement of time over the past 500,000 years, Earth and Planetary Science Letters, 81, 175–192, https://doi.org/10.1016/0012-821X(87)90154-3, 1987.

Edwards, R. L., Gallup, C. D., and Cheng, H.: Uranium-series dating of marine and lacustrine carbonates, in: Uranium-series geochemistry, edited by Bourdon, B., Turner, S., Henderson, G. M., and Lundstrom, C. C., vol. 52 of *Reviews in Mineralogy and Geochemistry*, pp. 363–405, Mineralogical Society of America, Washington, D.C., USA, ISBN 0-939950-54-5, 2003.

Engel, J. and Pickering, R.: The role of inherited Pb in controlling the quality of speleothem U–Pb ages, Quaternary Geochronology, 67, 101 243, https://doi.org/10.1016/j.quageo.2021.101243, 2022.

Engel, J., Maas, R., Woodhead, J., Tympel, J., and Greig, A.: A single-column extraction chemistry for isotope dilution U–Pb dating of carbonate, Chemical Geology, 531, 119 311, https://doi.org/10.1016/j.chemgeo.2019.119311, 2020.

Fairchild, I. J. and Baker, A.: Speleothem science: from process to past environments, Wiley-Blackwell, ISBN 978-1-4051-9620-8, 2012.

Fairchild, I. J., Smith, C. L., Baker, A., Fuller, L., Spötl, C., Mattey, D., McDermott, F., and F, E. I. M.: Modification and preservation of environmental signals in speleothems, Earth-Science Reviews, 75, 105–153, https://doi.org/10.1016/j.earscirev.2005.08.003, 2006.

Fujii, T., Moynier, F., and Albarède, F.: The nuclear field shift effect in chemical exchange reactions, Chemical Geology, 267, 139–156, https://doi.org/10.1016/j.chemgeo.2009.06.015, 2009.

Hajdas, I., Ascough, P., Garnett, M. H., Fallon, S. J., Pearson, C. L., Quarta, G., Spalding, K. L., Yamaguchi, H., and Yoneda, M.: Radiocarbon dating, Nat Rev Methods Primers, 1, 1–26, https://doi.org/10.1038/s43586-021-00058-7, 2021.

Hellstrom, J.: Rapid and accurate U/Th dating using parallel ion-counting multi-collector ICP-MS, Journal of Analytical Atomic Spectrometry, 18, 1346, https://doi.org/10.1039/b308781f, 2003.

https://doi.org/10.5194/egusphere-2024-3594
Preprint. Discussion started: 22 November 2024

Hellstrom, J. C.: Late Quaternary Palaeoenvironmental Records from the Geochemistry of Speleothems, North-West Nelson, New Zealand, Ph.D. thesis, Australian National University, Canberra, Australia, 1998.

Hiess, J., Condon, D. J., McLean, N., and Noble, S. R.: $^{238}U/^{235}U$ systematics in terrestrial uranium-bearing minerals, Science, https://doi.org/10.1126/science.1215507, 2012.

Isola, I., Zanchetta, G., Drysdale, R. N., Regattieri, E., Bini, M., Bajo, P., Hellstrom, J. C., Baneschi, I., Lionello, P., Woodhead, J., and Greig, A.: The 4.2 ka event in the central Mediterranean: new data from a Corchia speleothem (Apuan Alps, central Italy), Climate of the Past, 15, 135–151, https://doi.org/10.5194/cp-15-135-2019, 2019.

Jaffey, A. H., Flynn, K. F., Glendeni, L. E., Bentley, W. C., and Essling, A. M.: Precision measurement of half-lives and specific activities of U-235 and U-238, Physical Review C, 4, 1889–1906, 1971.

Klaus, J. S., Meeder, J. F., McNeill, D. F., Woodhead, J. F., and Swart, P. K.: Expanded Florida reef development during the mid-Pliocene warm period, Global and Planetary Change, 152, 27–37, https://doi.org/10.1016/j.gloplacha.2017.02.001, 2017.

Li, H. and Tissot, F. L. H.: UID: The uranium isotope database, Chemical Geology, 618, 121 221, https://doi.org/10.1016/j.chemgeo.2022.121221, 2023.

Ludwig, K. R.: Calculation of uncertainties of U-Pb isotope data, Earth and Planetary Science Letters, pp. 212–202, 1980.

Ludwig, K. R.: Mathematical–Statistical treatment of data and errors for $^{230}Th/U$ geochronology, in: Uranium-series geochemistry, edited by Bourdon, B., Turner, S., Henderson, G. M., and Lundstrom, C. C., vol. 52 of *Reviews in Mineralogy & Geochemistry*, pp. 631–656, Mineralogical Society of America, Washington, D.C., USA, ISBN 0-939950-54-5, 2003.

Ludwig, K. R. and Titterington, D. M.: Calculation of $^{230}Th/U$ isochrons, ages, and errors, Geochimica et Cosmochimica Acta, 58, 5031–5042, https://doi.org/10.1016/0016-7037(94)90229-1, 1994.

McLean, N. M., Smith, C. J., Roberts, N. M. W., and Richards, D. A.: Connecting the U–Th and U–Pb Chronometers: New Algorithms and Applications, in: AGU Fall Meeting, 2016.

Meckler, A. N., Clarkson, M. O., Cobb, K. M., Sodemann, H., and Adkins, J. F.: Interglacial hydroclimate in the tropical West Pacific through the Late Pleistocene., Science, 336, 1301–1304, https://doi.org/10.1126/science.1218340, 2012.

Meyer, M. C., Cliff, R. A., Spotl, C., Knipping, M., and Mangini, A.: Speleothems from the earliest Quaternary: Snapshots of paleoclimate and landscape evolution at the northern rim of the Alps, Quaternary Science Reviews, 28, 1374–1391, https://doi.org/10.1016/j.quascirev.2009.01.010, 2009.

Piccini, L., Zanchetta, G., Drysdale, R. N., Hellstrom, J., Isola, I., Fallick, A. E., Leone, G., Doveri, M., Mussi, M., Mantelli, F., Molli, G., Lotti, L., Roncioni, A., Regattieri, E., Meccheri, M., and Vaselli, L.: The environmental features of the Monte Corchia cave system (Apuan Alps, central Italy) and their effects on speleothem growth, International Journal of Speleology, 37, 153–172, https://doi.org/10.5038/1827-806X.37.3.2, 2008.

Pickering, R., Kramers, J. D., Partridge, T., Kodolanyi, J., and Pettke, T.: U-Pb dating of calcite-aragonite layers in speleothems from hominin sites in South Africa by MC-ICP-MS, Quaternary Geochronology, 5, 544–558, https://doi.org/10.1016/j.quageo.2009.12.004, 2010.

Pickering, R., Dirks, P. H. G. M., Jinnah, Z., de Ruiter, D. J., Churchill, S. E., Herries, A. I. R., Woodhead, J. D., Hellstrom, J. C., and Berger, L. R.: *Australopithecus sediba* at 1.977 Ma and implications for the origins of the genus Homo, Science, 333, 1421–1423, https://doi.org/10.1126/science.1203697, 2011.

Pollard, T., Woodhead, J., Hellstrom, J., Engel, J., Powell, R., and Drysdale, R.: DQPB: software for calculating disequilibrium U–Pb ages, Geochronology, 5, 181–196, https://doi.org/10.5194/gchron-5-181-2023, 2023.

https://doi.org/10.5194/egusphere-2024-3594
Preprint. Discussion started: 22 November 2024

Potter, E.-K., Stirling, C. H., Andersen, M. B., and Halliday, A. N.: High precision Faraday collector MC-ICPMS thorium isotope ratio determination, International Journal of Mass Spectrometry, 247, 10–17, https://doi.org/10.1016/j.ijms.2005.08.017, 2005.

Pythoud, M.: Development of High-Precision Measurements for Uranium and Thorium Isotopes Using a Multi-Collector- Inductively-Coupled Plasma Mass Spectrometer, Master's thesis, University of Minnesota, Minneapolis, USA, 2022.

Regattieri, E., Zanchetta, G., Drysdale, R. N., Isola, I., Hellstrom, J. C., and Dallai, L.: Late glacial to holocene trace element record (Ba, Mg, Sr) from Corchia Cave (Apuan Alps, central Italy): paleoenvironmental implications, Journal of Quaternary Science, 29, 381–392, https://doi.org/10.1002/jqs.2712, 2014.

Richards, D. A., Bottrell, S. H., Cliff, R. A., Ströhle, K., and Rowe, P. J.: U-Pb dating of a speleothem of Quaternary age, Geochimica et Cosmochimica Acta, 62, 3683–3688, https://doi.org/10.1016/S0016-7037(98)00256-7, 1998.

Richter, S., Eykens, R., Kühn, H., Aregbe, Y., Verbruggen, A., and Weyer, S.: New average values for the $n(^{238}U)/n(^{235}U)$ isotope ratios of natural uranium standards, International Journal of Mass Spectrometry, 295, 94–97, https://doi.org/10.1016/j.ijms.2010.06.004, 2010.

Roberts, N. M. W., Drost, K., Horstwood, M. S. A., Condon, D. J., Chew, D., Drake, H., Milodowski, A. E., McLean, N. M., Smye, A. J., Walker, R. J., Haslam, R., Hodson, K., Imber, J., Beaudoin, N., and Lee, J. K.: Laser ablation inductively coupled plasma mass spectrometry (LA-ICP-MS) U–Pb carbonate geochronology: strategies, progress, and limitations, Geochronology, 2, 33–61, https://doi.org/10.5194/gchron-2-33-2020, 2020.

Russell, W. A., Papanastassiou, D. A., and Tombrello, T. A.: Ca isotope fractionation on the Earth and other solar system materials, Geochimica et Cosmochimica Acta, 42, 1075–1090, https://doi.org/10.1016/0016-7037(78)90105-9, 1978.

Schaltegger, U., Ovtcharova, M., Gaynor, S. P., Schoene, B., Wotzlaw, J.-F., Davies, J. F. H. L., Farina, F., Greber, N. D., Szymanowski, D., and Chelle-Michou, C.: Long-term repeatability and interlaboratory reproducibility of high-precision ID-TIMS U–Pb geochronology, J. Anal. At. Spectrom., 36, 1466–1477, https://doi.org/10.1039/D1JA00116G, 2021.

Scholz, D., Hoffmann, D. L., Hellstrom, J., and Bronk Ramsey, C.: A comparison of different methods for speleothem age modelling, Quaternary Geochronology, 14, 94–104, https://doi.org/10.1016/j.quageo.2012.03.015, 2012.

Scholz, D., Tolzmann, J., Hoffmann, D. L., Jochum, K. P., Spötl, C., and Riechelmann, D. F. C.: Diagenesis of speleothems and its effect on the accuracy of ^{230}Th/U-ages, Chemical Geology, 387, 74–86, https://doi.org/10.1016/j.chemgeo.2014.08.005, 2014.

Shen, C.-C., Wu, C.-C., Cheng, H., Edwards, R. L., Hsieh, Y.-T., Gallet, S., Chang, C.-C., Li, T.-Y., Lam, D. D., Kano, A., Hori, M., and Spötl, C.: High-precision and high-resolution carbonate ^{230}Th dating by MC-ICP-MS with SEM protocols, Geochimica et Cosmochimica Acta, 99, 71–86, https://doi.org/10.1016/j.gca.2012.09.018, 2012.

Sniderman, J. M. K., Woodhead, J. D., Hellstrom, J., Jordan, G. J., Drysdale, R. N., Tyler, J. J., and Porch, N.: Pliocene reversal of late Neogene aridification, Proceedings of the National Academy of Sciences, 113, 1999–2004, https://doi.org/10.1073/pnas.1520188113, 2016.

Spötl, C. and Mangini, A.: Paleohydrology of a high-elevation, glacier-influenced karst system in the Central Alps (Austria), Austrian Journal of Earth Sciences, 103, 92–105, 2010.

Steiger, R. and Jäger, E.: Subcommission on geochronology: Convention on the use of decay constants in geo- and cosmochronology, Earth and Planetary Science Letters, 36, 359–362, https://doi.org/10.1016/0012-821X(77)90060-7, 1977.

Stirling, C. H., Andersen, M. B., Potter, E.-K., and Halliday, A. N.: Low-temperature isotopic fractionation of uranium, Earth and Planetary Science Letters, 264, 208–225, https://doi.org/10.1016/j.epsl.2007.09.019, 2007.

Szymanowski, D. and Schoene, B.: U–Pb ID-TIMS geochronology using ATONA amplifiers, J. Anal. At. Spectrom., 35, 1207–1216, https://doi.org/10.1039/D0JA00135J, 2020.

https://doi.org/10.5194/egusphere-2024-3594
Preprint. Discussion started: 22 November 2024

Tera, F. and Wasserburg, G. J.: U-Th-Pb systematics in three Apollo 14 basalts and the problem of initial Pb in lunar rocks, Earth and Planetary Science Letters, 14, 281–304, https://doi.org/10.1016/0012-821X(72)90128-8, 1972.

Tissot, F. L. H. and Dauphas, N.: Uranium isotopic compositions of the crust and ocean: Age corrections, U budget and global extent of modern anoxia, Geochimica et Cosmochimica Acta, 167, 113–143, https://doi.org/10.1016/j.gca.2015.06.034, 2015.

Tzedakis, P. C., Drysdale, R. N., Margari, V., Skinner, L. C., Menviel, L., Rhodes, R. H., Taschetto, A. S., Hodell, D. A., Crowhurst, S. J., Hellstrom, J. C., Fallick, A. E., Grimalt, J. O., McManus, J. F., Martrat, B., Mokeddem, Z., Parrenin, F., Regattieri, E., Roe, K., and Zanchetta, G.: Enhanced climate instability in the North Atlantic and southern Europe during the Last Interglacial, Nature Communications, 9, 1383–14, https://doi.org/10.1038/s41467-018-06683-3, 2018.

Vaks, A., Mason, A. J., Breitenbach, S. F. M., Kononov, A. M., Osinzev, A. V., Rosensaft, M., Borshevsky, A., Gutareva, O. S., and Henderson, G. M.: Palaeoclimate evidence of vulnerable permafrost during times of low sea ice, Nature, 577, 221–225, https://doi.org/10.1038/s41586-019-1880-1, 2020.

Walker, J., Cliff, R. A., and Latham, A. G.: U-Pb isotopic age of the StW 573 hominid from Sterkfontein, South Africa., Science, 314, 1592–1594, https://doi.org/10.1126/science.1132916, 2006.

Wang, X., Wang, X., Wang, L., Wu, S., Xue, D., Duan, W., Ma, Z., Xiao, J., and Li, X.: Uranium isotope ratios of twenty-nine geological rock reference materials measured by MC-ICP-MS, Geostandards and Geoanalytical Research, 47, 945–955, https://doi.org/10.1111/ggr.12501, 2023.

Wang, Y., Cheng, H., Edwards, R. L., Kong, X., Shao, X., Chen, S., Wu, J., Jiang, X., Wang, X., and An, Z.: Millennial- and orbital-scale changes in the East Asian monsoon over the past 224,000 years, Nature, 451, 1090–1093, https://doi.org/10.1038/nature06692, 2008.

Wendt, I. and Carl, C.: U/Pb dating of discordant 0.1 Ma old secondary U minerals, Earth and Planetary Science Letters, 73, 278–284, 1985.

Weyer, S., Anbar, A. D., Gerdes, A., Gordon, G. W., Algeo, T. J., and Boyle, E. A.: Natural fractionation of $^{238}U/^{235}U$, Geochimica et Cosmochimica Acta, 72, 345–359, https://doi.org/10.1016/j.gca.2007.11.012, 2008.

Woodhead, J. and Petrus, J.: Exploring the advantages and limitations of in situ U–Pb carbonate geochronology using speleothems, Geochronology, 1, 69–84, https://doi.org/10.5194/gchron-1-69-2019, 2019.

Woodhead, J. and Pickering, R.: Beyond 500 ka: Progress and prospects in the U–Pb chronology of speleothems, and their application to studies in palaeoclimate, human evolution, biodiversity and tectonics, Chemical Geology, 322–323, 290–299, https://doi.org/10.1016/j.chemgeo.2012.06.017, 2012.

Woodhead, J., Hellstrom, J., Maas, R., Drysdale, R., Zanchetta, G., Devine, P., and Taylor, E.: U–Pb geochronology of speleothems by MC-ICPMS, Quaternary Geochronology, 1, 208–221, https://doi.org/10.1016/j.quageo.2006.08.002, 2006.

Woodhead, J., Hellstrom, J., Pickering, R., Drysdale, R., Paul, B., and Bajo, P.: U and Pb variability in older speleothems and strategies for their chronology, Quaternary Geochronology, 14, 105–113, https://doi.org/10.1016/j.quageo.2012.02.028, 2012.

York, D., Evensen, N. M., Martínez, M. L., and De Basabe Delgado, J.: Unified equations for the slope, intercept, and standard errors of the best straight line, American Journal of Physics, 72, 367–375, https://doi.org/10.1119/1.1632486, 2004.

Zanchetta, G., Drysdale, R. N., Hellstrom, J. C., Fallick, A. E., Isola, I., Gagan, M. K., and Pareschi, M. T.: Enhanced rainfall in the Western Mediterranean during deposition of sapropel S1: stalagmite evidence from Corchia cave (Central Italy), Quaternary Science Reviews, 26, 279–286, https://doi.org/10.1016/j.quascirev.2006.12.003, 2007.

Zhong, Y.-T., Mundil, R., Xu, Y.-G., Wang, G.-Q., Zhang, Z.-F., and Ma, J.-L.: Development of CA-ID-TIMS zircon U–Pb dating technique at Guangzhou Institute of Geochemistry, Chinese Academy of Sciences, Solid Earth Sciences, 2, 55–61, https://doi.org/10.1016/j.sesci.2017.03.001, 2017.